

# Non-quasiconvex dispersion of composite fermions and the fermionic Haffnian state in the first-excited Landau level

Hao Jin<sup>1</sup> and Junren Shi<sup>1,2,\*</sup>

<sup>1</sup>*International Center for Quantum Materials, Peking University, Beijing 100871, China*

<sup>2</sup>*Collaborative Innovation Center of Quantum Matter, Beijing 100871, China*

It has long been puzzling that fractional quantum Hall states in the first excited Landau level (1LL) often differ significantly from their counterparts in the lowest Landau level. We show that the dispersion of composite fermions (CFs) is a deterministic factor driving the distinction. We find that CFs with two quantized vortices in the 1LL have a non-quasiconvex dispersion. Consequently, in the filling fraction  $7/3$ , CFs occupy the second  $\Lambda$ -level instead of the first. The corresponding ground state wave function, based on the CF wave function ansatz, is identified to be the fermionic Haffnian wave function rather than the Laughlin wave function. The conclusion is supported by numerical evidence from exact diagonalizations in both disk and spherical geometries. Furthermore, we show that the dispersion becomes quasiconvex in wide quantum wells or for CFs with four quantized vortices in the filling fraction  $11/5$ , coinciding with observations that the distinction between the Landau levels disappears under these circumstances.

*Introduction.*— A two-dimensional electron gas subjected to a strong perpendicular magnetic field exhibits the fractional quantum Hall effect (FQHE), characterized by fractionally quantized Hall plateaus in specific filling fractions of Landau levels [1, 2]. The effect is also observed in topological flat bands [3] in recent experiments [4–7]. Theoretical understanding of the FQHE is challenging because the kinetic energies of electrons in a Landau level are completely quenched, leaving interaction to dominate. Consequently, constructing plausible ground state wave functions for the FQHE has long relied on intuition or educated guesses, from the celebrated Laughlin wave function [8] to those hypothesized by more elaborate approaches such as the hierarchy theory [9, 10], the conformal field theory [11, 12], and the composite fermion (CF) theory [13, 14]. Among these, Jain’s CF theory is the most successful. The theory introduces fictitious particles called CFs, each consisting of an electron and an even number of quantized vortices. Wave functions prescribed by the CF theory yield nearly perfect overlaps with those obtained from exact diagonalizations (ED) in the lowest Landau level (LLL) [15–17]. Furthermore, it has been shown that a deductive approach for determining CF wave functions and corresponding physical wave functions can be established [18].

While the FQHE in the LLL can be well described by the CF theory, it has long been puzzling that the FQHE in the first excited Landau level (1LL) often exhibits distinct features. Most notably, a Hall plateau is developed in the even denominator fraction  $\nu = 5/2$  [19], which has been a focus in the pursuit of topological quantum computing [20]. On the other hand, ordinary fractions with odd denominators in the 1LL, such as  $\nu = 7/3$  and  $\nu = 12/5$ , differ significantly from their counterparts in the LLL [21–24]. The observation casts doubt on the applicability of the CF theory in the 1LL, motivating alternative pictures such as the parafermion theory [25] and the parton theory [26, 27].

A representative case is the filling fraction  $\nu = 7/3$  with an effective filling fraction  $\tilde{\nu} = 1/3$  in the 1LL [19, 21]. This state is expected to be an analog of the  $1/3$  state in the LLL and described by the  $1/3$  Laughlin wave function. However, it is found that the overlap between the  $1/3$  and  $7/3$  states is low [21, 24], and their entanglement and quasi-hole excitation spectra are distinct [28–30]. More puzzlingly, ED shows that the  $11/5$  state can nevertheless be well described by the  $1/5$  Laughlin wave function [21, 24]. Several theories had been put forward to explain the peculiarity of the  $7/3$  state. Töke *et al.* suggest that there exists substantial  $\Lambda$ -level mixing induced by residue interaction between CFs [24]. Balram *et al.* propose that the  $7/3$  state hosts  $\mathbb{Z}_n$ -superconductivity of partons [27]. Various trial wave functions for this fraction have been numerically tested in Refs. 22, 23, 31, 32.

In this Letter, we demonstrate that the dispersion of CFs is a key for understanding the peculiarities of the 1LL. Based on the deductive approach developed in Ref. 18, we show that CFs with two quantized vortices (denoted as  $\text{CF}^2$ ) in the 1LL, unlike CFs in the LLL, have a non-quasiconvex dispersion. Consequently, in  $\nu = 7/3$ , CFs occupy the second  $\Lambda$ -level [14] instead of the first. The corresponding ground state is identified to be the fermionic Haffnian state, also known as the  $d$ -wave paired FQH state of spinless electrons [33, 34], rather than the Laughlin state. Using ED, we demonstrate that the unique features of the Haffnian state do manifest in exact ground state wave functions. Furthermore, we find that the dispersion becomes quasiconvex in wide quantum wells or for  $\text{CF}^4$  in the  $11/5$  state, coinciding with observations that the distinction between the 1LL and LLL disappears under these circumstances. These findings, cumulatively, support that the non-quasiconvex CF dispersion is a deterministic factor behind the peculiarities of the FQHE in the 1LL.

*CF dispersion.*— A CF consists of an electron and a vortex carrying an even number of quantized vortices.

The Coulomb attraction between the electron and the charge void induced by the vortex gives rise to the binding energy of the CF [18]. Read shows that the momentum of a CF can be defined as being proportional to the spatial separation between the electron and vortex [35]. Consequently, the binding energy, as a function of the spatial separation  $r$ , can be interpreted as the dispersion of the CF [36]. To determine the binding energy, we first calculate the electron-vortex correlation function  $h(r)$ , which describes the electron density profile in the vicinity of a vortex. The binding energy can then be determined by  $\epsilon_b(r) = (\rho_0/2) \int d^2\mathbf{r}' v(|\mathbf{r} - \mathbf{r}'|)h(r')$ , where  $v(r)$  is the interaction between electrons and  $\rho_0$  is the average electron density [18].

We can determine  $h(r)$  for  $\text{CF}^2$  by assuming the ground state to be the  $1/3$  Laughlin state. The many-body wave function in the presence of a vortex at the origin is given by  $\Psi_0^v(\{z_i\}) = \prod_i z_i^2 \prod_{i<j} (z_i - z_j)^3$ , where  $\{z_i = x_i + iy_i\}$  is the set of complex electron coordinates [18].  $h(r)$  is obtained by computing the electron density distribution of  $\Psi_0^v$  normalized by  $\rho_0$ . The result is shown in the inset of Fig. 1.

Different interactions  $v(r)$  give rise to different binding energies of  $\text{CF}^2$  for the LLL and the 1LL. For the LLL,  $v(r)$  is the Coulomb interaction  $v_c(r) = e^2/4\pi\epsilon r$ . For the 1LL, we map the problem of interacting electrons to the mathematically equivalent problem of interacting electrons in the LLL with the effective interaction [14]:

$$\tilde{v}(r) = \left(1 + \frac{l_B^2 \nabla^2}{2}\right)^2 v_c(r), \quad (1)$$

where  $l_B = \sqrt{\hbar/eB}$  is the magnetic length with  $B$  being the strength of the magnetic field. The binding energy of  $\text{CF}^2$  in the LLL and 1LL can then be determined using  $h(r)$  and the respective interactions. The results are shown in Fig. 1. We observe that the binding energy of  $\text{CF}^2$  in the 1LL, unlike that in the LLL, is a non-quasiconvex function of  $r$ .

*$\Lambda$  levels and wave functions.*— With the binding energy of a CF, we can establish its effective Hamiltonian. In the dipole picture, the electron and vortex in a CF are confined in two separate LLLs induced by the physical magnetic field and the emergent Chern-Simons magnetic field, respectively [18]. As a result, the CF is described by a bi-variate wave function  $\psi(z, \bar{\eta})$ , which is (anti-)holomorphic in the complex electron (vortex) coordinate  $z$  ( $\eta \equiv \eta_x + i\eta_y$ ). After projecting to the LLLs,  $\bar{z}$  and  $\eta$  become the operators  $\hat{z} = 2l_B^2 \partial_z$  and  $\hat{\eta} = 2l_b^2 \partial_{\bar{\eta}}$ , respectively, where  $l_b = l_B/\sqrt{2\tilde{\nu}}$  is the magnetic length of Chern-Simons magnetic field for  $\text{CF}^2$  [14, 18]. We can then define the ladder operators of  $\Lambda$ -levels as  $\hat{a} = (z - \hat{\eta})/\sqrt{\gamma}l_B$  and  $\hat{a}^\dagger = (\hat{z} - \bar{\eta})/\sqrt{\gamma}l_B$ , with  $\gamma \equiv |1/\tilde{\nu} - 2| = 1/q$  for the filling fraction  $\tilde{\nu} = q/(2q + 1)$ . The effective Hamiltonian operator of the CF is given

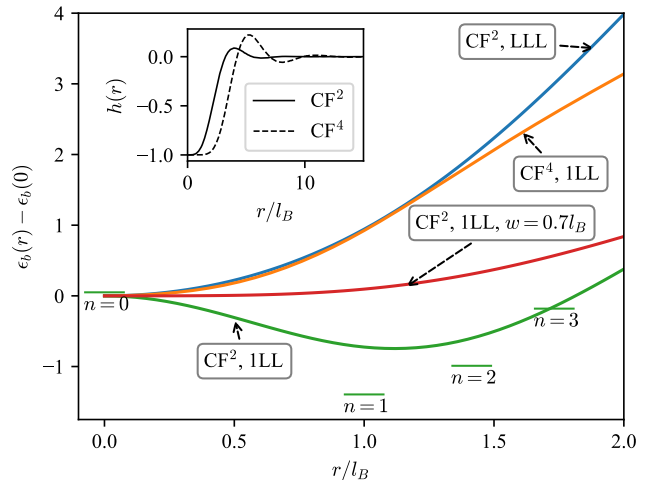


FIG. 1: Binding energy  $\epsilon_b(r)$  for  $\text{CF}^2$  and  $\text{CF}^4$  in the LLL and 1LL. The binding energy of  $\text{CF}^2$  in the 1LL in a quantum well with a finite width  $w = 0.7l_B$  is also shown. The horizontal line segments indicate the energies of  $\Lambda$ -levels for  $\nu = 7/3$ . The energies are in units of  $\tilde{\nu}e^2/16\pi^2\epsilon l_B$ . Inset: electron-vortex correlation function  $h(r)$  for  $\text{CF}^2$  and  $\text{CF}^4$ .

by:

$$\hat{H} =: \epsilon_b(\hat{r}) :, \quad (2)$$

where we express the binding energy as a function of  $r^2 \equiv |z - \eta|^2$ , which is then mapped to the operator  $\hat{r}^2 \equiv \gamma l_B^2 \hat{a}^\dagger \hat{a}$ . The colons indicate the normal ordering of the ladder operators, which places  $\hat{a}^\dagger$ 's to the left of  $\hat{a}$ 's. The specific ordering of the ladder operators is a result of the particular way that the binding energy is defined [18].

The eigen-energies and eigen-states of  $\hat{H}$  can be determined. It is easy to see that the number operator  $\hat{n} \equiv \hat{a}^\dagger \hat{a}$  commutes with the Hamiltonian:  $[\hat{H}, \hat{n}] = 0$ . We can thus define the index of  $\Lambda$ -levels as the eigenvalue of  $\hat{n}$ . Similar to ordinary Landau levels, wave functions for the first ( $n = 0$ )  $\Lambda$ -level is annihilated by the lowering operator  $\hat{a}$ . We thus have  $\psi_0(z, \bar{\eta}) = f(z) \exp(z\bar{\eta}/2l_b^2)$ , where  $f(z)$  is a holomorphic function in  $z$ . Wave functions for  $n > 0$  can be obtained by successively applying the raising operator to  $\psi_0(z, \bar{\eta})$ :  $\psi_n(z, \bar{\eta}) = (\hat{a}^\dagger)^n / \sqrt{n!} \psi_0(z, \bar{\eta})$ . The energies of  $\Lambda$ -levels as a function of  $n$  can be determined straightforwardly [37]. The result for  $\nu = 7/3$  is shown in Fig. 1. Notably, the lowest  $\Lambda$ -level has the index  $n = 1$  rather than  $n = 0$ .

The physical wave function of the  $7/3$  state can be determined by applying the wave function ansatz of the CF theory, which maps a many-body wave function of CFs to a physical wave function of electrons. From the energy spectrum of  $\Lambda$ -levels, we expect that CFs in the  $7/3$  state fully occupy the second  $\Lambda$ -level. The corresponding wave function of CFs can be obtained by applying raising operators to the wave function  $\Psi_{\text{CF}}^0(\{z_i, \bar{\eta}_i\})$  of a fully occupied first

$\Lambda$ -level:  $\Psi_{\text{CF}}(\{z_i, \bar{\eta}_i\}) \propto \prod_i (2l_B^2 \partial_{z_i} - \bar{\eta}_i) \Psi_{\text{CF}}^0(\{z_i, \bar{\eta}_i\})$ , with  $\Psi_{\text{CF}}^0(\{z_i, \bar{\eta}_i\}) \equiv \prod_{i < j} (z_i - z_j) \exp(\sum_i z_i \bar{\eta}_i / 2l_B^2)$ . The electron wave function can then be obtained by overlapping  $\Psi_{\text{CF}}$  with the  $1/2$  Laughlin state of vortices [18]. We obtain [38]:

$$\Psi(\{z_i\}) \propto \lim_{\eta \rightarrow z} \prod_i (2\partial_{z_i} - \partial_{\eta_i}) \prod_{i < j} (z_i - z_j) (\eta_i - \eta_j)^2. \quad (3)$$

We can obtain an explicit form of the wave function [38]. For an even number of electrons, it is the fermionic Haffnian wave function [33, 39, 40]:

$$\Psi(\{z_i\}) \propto \text{Hf} \left[ \frac{1}{(z_i - z_j)^2} \right] \prod_{i < j} (z_i - z_j)^3, \quad (4)$$

where Hf denotes the Haffnian of a matrix with off-diagonal elements  $1/(z_i - z_j)^2$ . The specific Haffnian can also be written as the determinant  $\det[1/(z_i - z_j)]$  [39]. For an odd number of electrons, on the other hand, the wave function Eq. (3) predicted by the CF theory is identically zero [41]. The Haffnian state was first proposed as a  $d$ -wave pairing state analogous to the  $p$ -wave Pfaffian state [33]. As far as we know, this is the first time that the state is related to the CF theory, with the underlying CF state identified.

Similarly, we can determine the  $\Lambda$ -levels for the filling fraction  $\nu = 12/5$  with the effective filling fraction  $\tilde{\nu} = 2/5$  in the 1LL. In this case, we find that the two lowest  $\Lambda$ -levels have the indices  $n = 2, 3$  [38]. Consequently, CFs in the  $12/5$  state occupy the third and fourth  $\Lambda$ -levels rather than the first two as in the  $2/5$  state. The resulting electron state should also differ significantly from the  $2/5$  state in the LLL.

*Numerical verification.*— Using ED, we test our conclusion for  $\nu = 7/3$  by examining whether features of the Haffnian state manifest in exact ground state wave functions. Compared to the Laughlin state, the Haffnian state has a smaller  $z$ -component of the total angular momentum  $L_z$  on a disk and a different topological shift  $S$  on a sphere. Moreover, the pairing nature of the state suggests stability only for even numbers of electrons. We therefore solve the ground state wave functions of interacting electrons in both the disk and spherical geometries. The results corroborate our conclusion well.

In the disk geometry,  $L_z$  of the Haffnian state Eq. (4) is smaller than that of the Laughlin state by  $N$ , where  $N$  is the number of electrons. Figure 2 shows the lowest eigen-energies in different  $L_z$  sectors for  $\nu = 1/3$  and  $7/3$ . It is evident that the exact ground states for  $\nu = 7/3$  do have the  $L_z$  values expected for the Haffnian state for  $N \geq 10$ . For  $N = 8$ , we observe a deviation by one, likely due to finite size effects.

In the spherical geometry, the Haffnian state has a different topological shift  $S$  compared to the Laughlin state. The topological shift  $S$  is defined by the relation  $2l \equiv \tilde{\nu}^{-1}N - S$ , where  $l$  is the angular-momentum

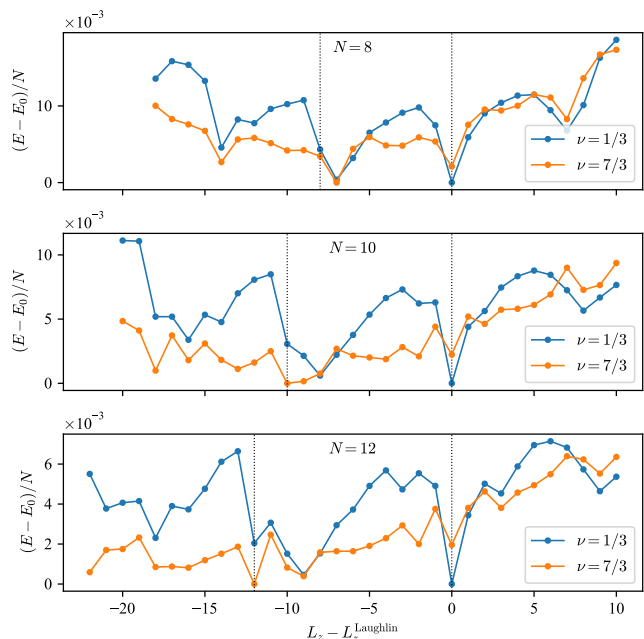


FIG. 2: Lowest ED energies per particle of  $\nu = 1/3$  and  $\nu = 7/3$  in different  $L_z$  sectors.  $E_0$  denotes the ground state energy. The energies are in units of  $e^2/4\pi\epsilon l_B$ .  $L_z^{\text{Laughlin}} = 3N(N-1)/2$  denotes the  $z$  component of the total angular momentum of the Laughlin state. The vertical dashed lines indicate the values expected for the Haffnian state  $L_z^{\text{Haffnian}} = L_z^{\text{Laughlin}} - N$ .

quantum number of the physical Landau level [42]. For  $\text{CF}^2$ , we have  $l = l^* + (N-1)$ , where  $l^*$  is the angular-momentum quantum number of the first  $\Lambda$ -level [9, 14]. Fully occupying a  $\Lambda$ -level with the index  $n$  requires  $N = 2(l^* + n) + 1$ . Combining these relations, we have  $S = 3$  and  $S = 5$  for the Laughlin state ( $n = 0$ ) and the Haffnian state ( $n = 1$ ), respectively.

While  $S$  is a free parameter for ED calculations in the spherical geometry, its probable value could be identified by examining the degeneracies and stability (excitation gaps) of the ground states with respect to different values of  $S$  and  $N$ . For the  $7/3$  state, Wójs *et al.* investigated a few candidate values of  $S$  and concluded that  $S = 7$  is the most probable, based on the reasoning that for the particular shift, a gaped non-degenerate ground state with a total angular momentum  $L = 0$  can always be found for all calculated values of  $N$  [22, 23].  $S = 5$  was ruled out because the ground states become degenerate ( $L > 0$ ) for odd numbers of electrons.

To this end, we repeat the calculation and extend it for larger values of  $N$ . In Fig. 3, we show the  $N$  dependence of the excitation gaps for non-degenerate ground states at  $S = 3, 5, 7$ . Our calculation confirms Wójs *et al.*'s observation that the excitation gap for  $S = 7$  diminishes rapidly with increasing  $N$  for  $N \leq 12$ . When  $N$  is further increased, we observe that the ground states become

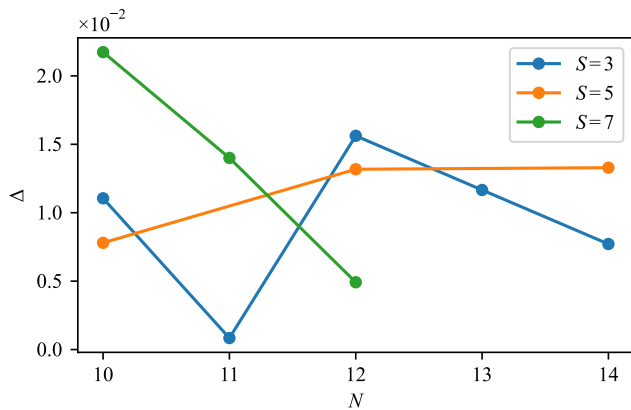


FIG. 3: Excitation gaps for non-degenerate ground states at  $S = 3, 5, 7$ , in units of  $e^2/4\pi\epsilon l_B$ .

degenerate. Conversely, although the ground states for  $S = 5$  are non-degenerate only for even numbers of electrons, the magnitude of the excitation gap shows a trend of converging to a constant value for  $N \geq 12$ , suggesting robustness of the non-degenerate ground states for  $S = 5$ .

In retrospect, we believe that the odd-even alternation observed in the ED results for  $S = 5$  should be interpreted as a manifestation of the pairing nature of the Haffnian state, rather than a reason to dismiss it. Remarkably, the CF theory, which projects the ground state of CFs for odd  $N$  to zero identically [41], predicts the alternation. With the CF ground state annihilated, the low-lying excited states of CFs are expected to generate both the ground state and low-lying excited states of electrons for odd  $N$  with  $S = 5$ . In Fig. 4, we present the low-lying electron energy spectrum for  $S = 5$ . We do observe that the spectrum for odd  $N$  bears resemblance to the excited portion of the spectrum for even  $N$ .

*Non-quasiconvex to quasiconvex transition.*— To further corroborate that the dispersion of CFs is a deterministic underlying factor, we investigate two scenarios under which the CF dispersion in the 1LL becomes quasiconvex. We anticipate that the distinction between the 1LL and LLL should disappear when the dispersion becomes quasi-convex. This is indeed observed.

The first scenario involves a different  $h(r)$ . We consider  $CF^4$ , which carries four quantized vortices and underlies the filling fraction  $11/5$ . In this case, the binding energy can be determined similarly to  $CF^2$ , albeit using the wave function  $\Psi_0^y(\{z_i\}) = \prod_i z_i^4 \prod_{i<j} (z_i - z_j)^5$ . We find that the resulting binding energy is a quasiconvex function of  $r$ , similar to that of  $CF^2$  in the LLL, as shown in Fig. 1. This is consistent with the fact that the  $11/5$  state can be well described by the Laughlin wave function [21, 24].

The second scenario involves the change of the electron interaction  $v(r)$ . We adopt the modified Coulomb interaction investigated in Ref. 43:  $v_c(r) = e^2/4\pi\epsilon\sqrt{r^2 + w^2}$ ,

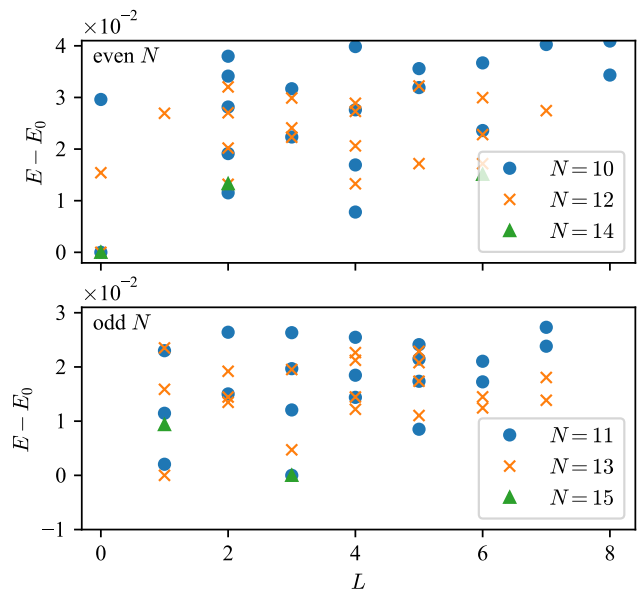


FIG. 4: ED spectrum for even and odd numbers of electrons.  $E_0$  denotes the ground state energy. The energies are in units of  $e^2/4\pi\epsilon l_B$ . For  $N = 14$  ( $N = 15$ ), only three (two) lowest levels are shown.

where  $w$  is a parameter for characterizing the width of the quantum well confining the two-dimensional system. We find that for  $CF^2$  in the 1LL, the dispersion becomes quasiconvex for  $w \gtrsim 0.7l_B$ , as shown in Fig. 1. This is consistent with the ED results of Ref. 43, which show that the overlap between the exact ground state wave function of the  $7/3$  state and the  $1/3$  Laughlin wave function approaches unity for  $w \gtrsim l_B$ .

*Summary and discussion.*— In summary, we show that CF dispersion is a deterministic factor behind the peculiarities of the FQHE in the 1LL. The deductive approach enables us to not only explain the distinction between the  $7/3$  or  $12/5$  states and their counterparts in the LLL, but also correctly predict the evolution of electron states under varying conditions.

Remarkably, the Haffnian state, considered analogous to the Pfaffian pairing state, can be linked to a non-interacting CF state. The non-interacting nature also suggests that quasi-electron or hole excitations of such a Haffnian ground state should resemble those of the Laughlin state [44], rather than those expected from conformal field theory and model Hamiltonian considerations [34, 45]. This interpretation seems to be consistent with the results of tunneling measurements [46, 47].

We need to point out that the single-particle mean-field approach employed in this study may not be adequate in fully capturing quantitative details of a state with strong pairing correlations, as in the case of the Haffnian state. Numerically, the overlap between the Haffnian wave function and the exact ground state wave function for  $\nu = 7/3$

is found to be moderate [32]. The pairing correlations also complicate the self-consistent determinations of the electron-vortex correlation function and the CF dispersion [38]. Nevertheless, as pointed out in Ref. 14, it is not uncommon for a qualitatively correct wave function to yield a low overlap with the exact wave function. It is reasonable to expect that considering the residual interaction between CFs could improve the quantitative agreement [24, 48].

We acknowledge B. Yang and X. Lin for useful discussions. This work is supported by the National Key R&D Program of China under Grand No. 2021YFA1401900 and the National Science Foundation of China under Grant No. 12174005.

---

\* Electronic address: junrenshi@pku.edu.cn

- [1] D. C. Tsui, H. L. Stormer, and A. C. Gossard, Phys. Rev. Lett. **48**, 1559 (1982).
- [2] H. L. Stormer, Rev. Mod. Phys. **71**, 875 (1999).
- [3] T. Neupert, C. Chamon, T. Iadecola, L. H. Santos, and C. Mudry, Physica Scripta **2015**, 014005 (2015).
- [4] J. Cai, E. Anderson, C. Wang, X. Zhang, X. Liu, W. Holtzmann, Y. Zhang, F. Fan, T. Taniguchi, K. Watanabe, *et al.*, Nature **622**, 63 (2023).
- [5] H. Park, J. Cai, E. Anderson, Y. Zhang, J. Zhu, X. Liu, C. Wang, W. Holtzmann, C. Hu, Z. Liu, T. Taniguchi, K. Watanabe, J.-H. Chu, T. Cao, L. Fu, W. Yao, C.-Z. Chang, D. Cobden, D. Xiao, and X. Xu, Nature **622**, 74 (2023).
- [6] F. Xu, Z. Sun, T. Jia, C. Liu, C. Xu, C. Li, Y. Gu, K. Watanabe, T. Taniguchi, B. Tong, J. Jia, Z. Shi, S. Jiang, Y. Zhang, X. Liu, and T. Li, Phys. Rev. X **13**, 031037 (2023).
- [7] Y. Zeng, Z. Xia, K. Kang, J. Zhu, P. Knüppel, C. Vaswani, K. Watanabe, T. Taniguchi, K. F. Mak, and J. Shan, Nature **622**, 69 (2023).
- [8] R. B. Laughlin, Phys. Rev. Lett. **50**, 1395 (1983).
- [9] F. D. M. Haldane, Phys. Rev. Lett. **51**, 605 (1983).
- [10] B. I. Halperin, Phys. Rev. Lett. **52**, 1583 (1984).
- [11] G. Cristofano, G. Maiella, R. Musto, and F. Nicodemi, Phys. Lett. B **262**, 88 (1991).
- [12] S. Fubini, Mod. Phys. Lett. A **06**, 347 (1991).
- [13] J. K. Jain, Phys. Rev. Lett. **63**, 199 (1989).
- [14] J. K. Jain, *Composite fermions* (Cambridge University Press, 2007).
- [15] G. Dev and J. K. Jain, Phys. Rev. B **45**, 1223 (1992).
- [16] X. G. Wu, G. Dev, and J. K. Jain, Phys. Rev. Lett. **71**, 153 (1993).
- [17] J. K. Jain and R. K. Kamilla, Int. J. Mod. Phys. B **11**, 2621 (1997).
- [18] J. Shi, Phys. Rev. Res. **6**, 023306 (2024).
- [19] R. Willett, J. P. Eisenstein, H. L. Störmer, D. C. Tsui, A. C. Gossard, and J. H. English, Phys. Rev. Lett. **59**, 1776 (1987).
- [20] C. Nayak, S. H. Simon, A. Stern, M. Freedman, and S. Das Sarma, Rev. Mod. Phys. **80**, 1083 (2008).
- [21] N. d'Ambrumenil and A. Reynolds, J. Phys. C **21**, 119 (1988).
- [22] A. Wójs, Phys. Rev. B **63**, 125312 (2001).
- [23] A. Wójs and J. J. Quinn, Physica E **12**, 63 (2002).
- [24] C. Töke, M. R. Peterson, G. S. Jeon, and J. K. Jain, Phys. Rev. B **72**, 125315 (2005).
- [25] N. Read and E. Rezayi, Phys. Rev. B **59**, 8084 (1999).
- [26] J. K. Jain, Phys. Rev. B **40**, 8079 (1989).
- [27] A. C. Balram, J. K. Jain, and M. Barkeshli, Phys. Rev. Res. **2**, 013349 (2020).
- [28] M. P. Zaletel, R. S. K. Mong, F. Pollmann, and E. H. Rezayi, Phys. Rev. B **91**, 045115 (2015).
- [29] A. C. Balram, Y.-H. Wu, G. J. Sreejith, A. Wójs, and J. K. Jain, Phys. Rev. Lett. **110**, 186801 (2013).
- [30] S. Johri, Z. Papić, R. N. Bhatt, and P. Schmitteckert, Phys. Rev. B **89**, 115124 (2014).
- [31] J.-S. Jeong, H. Lu, K. H. Lee, K. Hashimoto, S. B. Chung, and K. Park, Phys. Rev. B **96**, 125148 (2017).
- [32] B. Kuśmierz and A. Wójs, Phys. Rev. B **97**, 245125 (2018).
- [33] X.-G. Wen and Y.-S. Wu, Nucl. Phys. B. **419**, 455 (1994).
- [34] B. Yang, Phys. Rev. B **103**, 115102 (2021).
- [35] N. Read, Semicond. Sci. Technol. **9**, 1859 (1994).
- [36] G. Ji and J. Shi, Phys. Rev. Research **3**, 043055 (2021).
- [37] J. König and A. Hucht, SciPost Phys. **10**, 007 (2021).
- [38] See supplemental material.
- [39] M. Greiter, X.-G. Wen, and F. Wilczek, Nucl. Phys. B. **374**, 567 (1992).
- [40] D. Green, *Strongly Correlated States in Low Dimensions*, Ph.D. thesis, Yale University (2001), arXiv:cond-mat/0202455 .
- [41] X. G. Wu and J. K. Jain, Phys. Rev. B **51**, 1752 (1995).
- [42] X. G. Wen and A. Zee, Phys. Rev. Lett. **69**, 953 (1992).
- [43] Z. Papić, N. Regnault, and S. Das Sarma, Phys. Rev. B **80**, 201303 (2009).
- [44] C. Töke and J. K. Jain, Phys. Rev. B **80**, 205301 (2009).
- [45] M. Hermanns, N. Regnault, B. A. Bernevig, and E. Ardonne, Phys. Rev. B **83**, 241302 (2011).
- [46] M. Dolev, Y. Gross, Y. C. Chung, M. Heiblum, V. Umansky, and D. Mahalu, Phys. Rev. B **81**, 161303 (2010).
- [47] S. Baer, C. Rössler, T. Ihn, K. Ensslin, C. Reichl, and W. Wegscheider, Phys. Rev. B **90**, 075403 (2014).
- [48] H. Q. Trung and B. Yang, Phys. Rev. Lett. **127**, 046402 (2021).

# Supplemental Material for Non-quasiconvex dispersion of composite fermions and the fermionic Hafnian state in the first-excited Landau level

Hao Jin<sup>1</sup> and Junren Shi<sup>1,2</sup>

<sup>1</sup>International Center for Quantum Materials, Peking University, Beijing 100871, China

<sup>2</sup>Collaborative Innovation Center of Quantum Matter, Beijing 100871, China

## I. NOTATIONS

### A. Bergman space

A wave function in the LLL can generally be written as  $\psi(z) \exp(-|z|^2/4l_B^2)$ , where  $\psi(z)$  is a holomorphic function of the particle coordinate  $z \equiv x + iy$ , and  $l_B \equiv \sqrt{\hbar/eB}$  denotes the magnetic length.

Since the Gaussian factor is common for all states in the LLL, it is convenient to represent the states using only the holomorphic part of the wave function. In this work, the term “wave function” always refers to the holomorphic part, i.e.,  $\psi(z)$ .

All normalizable holomorphic wave functions form a Bergman space. The inner product in the space is defined as

$$\langle \psi_1 | \psi_2 \rangle = \int d\mu_B(\mathbf{z}) \psi_1^*(z) \psi_2(z), \quad (\text{S1})$$

where the integral measure is given by

$$d\mu_B(\mathbf{z}) \equiv \frac{d^2\mathbf{z}}{2\pi l_B^2} \exp(-|z|^2/2l_B^2). \quad (\text{S2})$$

The measure has a Gaussian weight, which compensates for the Gaussian factors omitted in the holomorphic wave functions.

### B. Reproducing kernel

One can define the reproducing kernel

$$K_B(z, \bar{\xi}) = e^{z\bar{\xi}/2l_B^2}, \quad (\text{S3})$$

which is essentially the coordinate representation of the identity operator as well as the projection operator of the Bergman space. The following identities hold

$$\int d\mu_B(\xi) K_B(z, \bar{\xi}) f(\xi) = f(z), \quad (\text{S4})$$

$$\int d\mu_B(\xi) K_B(z, \bar{\xi}) \bar{\xi}^k f(\xi) = (2l_B^2 \partial_z)^k f(z). \quad (\text{S5})$$

The second identity defines the projection of  $\bar{z}$  onto the LLL, underlying the well known rule  $\bar{z} \rightarrow 2l_B^2 \partial_z$  [1].

### C. Dipole picture

In the dipole picture, a CF is interpreted as a composite particle consisting of an electron and a vortex. While the electron is confined in the physical Landau level, the vortex is assumed to reside in a separate, fictitious Landau level generated by a Chern-Simons magnetic field oriented in the opposite direction of the physical magnetic field. The magnetic length of the fictitious Landau level,  $l_b$ , is related to  $l_B$  by

$$\frac{1}{l_b^2} = \frac{2\tilde{\nu}}{l_B^2}. \quad (\text{S6})$$

Further details of the dipole picture can be found in Ref. 2.

We can also define a Bergman space as well as its reproducing kernel for the fictitious Landau level:

$$d\mu_b(\boldsymbol{\eta}) \equiv \frac{d^2\boldsymbol{\eta}}{2\pi l_b^2} \exp\left(-|\boldsymbol{\eta}|^2/2l_b^2\right), \quad (\text{S7})$$

$$K_b(\bar{\eta}, \zeta) = e^{\bar{\eta}\zeta/2l_b^2}. \quad (\text{S8})$$

The state of a composite fermion is thus described by a bivariate wave function  $\psi(z, \bar{\eta})$ , which depends on the complex electron coordinate  $z$  and the complex-conjugate vortex coordinate  $\bar{\eta} \equiv \eta_x - i\eta_y$ .

## II. FROM THE CF BINDING ENERGY TO THE HAFFNIAN WAVE FUNCTION

In this section, we supplement the details of the derivation from the CF binding energy to the physical wave function of electrons.

### A. Binding energy

The CF binding energy  $\epsilon_b(r)$ , determined in the main text, is introduced in Sec. VB of Ref. 2. It is defined such that the energy functional of a CF can be written as

$$E = \int d\mu_B(\mathbf{z}) d\mu_b(\boldsymbol{\eta}) \psi^*(z, \bar{\eta}) \int d\mu_b(\boldsymbol{\eta}') e^{\bar{\eta}\eta'/2l_b^2} \epsilon_b(\mathbf{z}; \bar{\eta}, \eta') \psi(z, \bar{\eta}'), \quad (\text{S9})$$

where  $\epsilon_b(\mathbf{z}; \bar{\eta}, \eta')$  is obtained from  $\epsilon_b(r)$  through analytic continuation by interpreting  $r^2 \equiv |\mathbf{z} - \boldsymbol{\eta}|^2$  as  $(\bar{z} - \bar{\eta})(z - \eta')$ .

### B. Wave equation

The CF wave equation can be derived by applying the variational principle of quantum mechanics. By minimizing the energy functional Eq. (S9) with respect to  $\psi^*(z, \bar{\eta})$ , subject to the normalization constraint  $\int d\mu_B(\mathbf{z}) d\mu_b(\boldsymbol{\eta}) |\psi(z, \bar{\eta})|^2 = 1$ , we obtain

$$\epsilon\psi(z, \bar{\eta}) = \hat{H}\psi(z, \bar{\eta}), \quad (\text{S10})$$

where the Hamiltonian is given by

$$\left[ \hat{H}\psi \right] (z, \bar{\eta}) = \hat{P}' \epsilon_b(\mathbf{z}; \bar{\eta}, \eta') \psi(z, \bar{\eta}) \quad (\text{S11})$$

$$\equiv \int d\mu_B(\mathbf{z}') d\mu_b(\boldsymbol{\eta}') \exp\left(\frac{z\bar{z}'}{2l_B^2}\right) \exp\left(\frac{\bar{\eta}\eta'}{2l_b^2}\right) \epsilon_b(\mathbf{z}'; \bar{\eta}, \eta') \psi(z', \bar{\eta}'), \quad (\text{S12})$$

where  $\hat{P}'$  denotes the projection onto the physical and fictitious Landau levels. It maps  $\bar{z}$  and  $\eta'$  in  $\epsilon_b(\mathbf{z}, \bar{\eta}, \eta')$  to the operators  $\hat{z} \equiv 2l_B^2 \partial_z$  and  $\hat{\eta} \equiv 2l_b^2 \partial_{\bar{\eta}}$ , respectively.

The ordering of operators after the mapping is dictated by the definition of the projection explicitly given in Eq. (S12). We see that the projections for  $\mathbf{z}$  and  $\boldsymbol{\eta}$  take different forms, corresponding to the normal ordering and the anti-normal ordering defined in Appendix B of Ref. 2, respectively. Consequently, after the projection,  $\hat{z} - \bar{\eta}$  should always be placed to the left of  $z - \eta'$ .

The rules for promoting the binding energy  $\epsilon_b(r)$  to the Hamiltonian  $\hat{H}$  are summarized as follows:

- Express  $\epsilon_b(r)$  as a function of  $r^2$ ;
- Replace  $r^2$  with the operator  $(2l_B^2 \partial_z - \bar{\eta})(z - 2l_b^2 \partial_{\bar{\eta}})$ ;
- Rearrange operators so that all  $(2l_B^2 \partial_z - \bar{\eta})$ 's are to the left of  $(z - 2l_b^2 \partial_{\bar{\eta}})$ 's.

### C. Ladder operators and $\Lambda$ levels

Ladder operators for CF  $\Lambda$  levels, analogues to the ladder operators in ordinary Landau levels, can be defined as

$$\hat{a} = \frac{1}{\sqrt{\gamma}l_B} (z - 2l_b^2 \partial_{\bar{\eta}}), \quad (\text{S13})$$

$$\hat{a}^\dagger = \frac{1}{\sqrt{\gamma}l_B} (2l_B^2 \partial_z - \bar{\eta}), \quad (\text{S14})$$

for a filling factor  $\tilde{\nu} < 1/2$ . It is straightforward to verify the commutation relation  $[\hat{a}, \hat{a}^\dagger] = 1$ . Additionally, one can define operators  $\hat{b}$  and  $\hat{b}^\dagger$  to commute with  $\hat{a}$  and  $\hat{a}^\dagger$  and relate different states within a  $\Lambda$ -level. For further details, see Appendix A of Ref. 2.

Hamiltonian  $\hat{H}$  can then be expressed in terms of  $\hat{a}$  and  $\hat{a}^\dagger$  by mapping  $r^2$  to  $\gamma l_B^2 \hat{a}^\dagger \hat{a}$  in the binding energy function  $\epsilon_b(r)$ , and arranging  $\hat{a}$  and  $\hat{a}^\dagger$  operators according to normal ordering. It yields Eq. (2) of the main text.

It is straightforward to verify that the Hamiltonian  $\hat{H}$  commutes with the number operator  $\hat{n} = \hat{a}^\dagger \hat{a}$ . Consequently,  $\Lambda$ -levels can be defined as the eigen-states of the number operator and labeled by its eigen-values.

### D. Energies of $\Lambda$ levels

It is straightforward to determine the energies of  $\Lambda$  levels by expressing  $\epsilon_b(r)$  as a polynomial in  $r^2$ . Following the rules outlined above, we make the substitution

$$r^{2k} \rightarrow (\gamma l_B^2)^k \hat{a}^\dagger k \hat{a}^k = (\gamma l_B^2)^k \hat{n}(\hat{n} - 1) \cdots (\hat{n} - k + 1) \quad (\text{S15})$$

to promote the polynomial to a CF Hamiltonian. It results in a Hamiltonian that is a function of  $\hat{n}$  [3]. The eigen-energy of a  $\Lambda$ -level can then be obtained by substituting  $\hat{n}$  in the Hamiltonian with the  $\Lambda$ -level index  $n$ .

### E. Single-particle CF wave functions

The wave functions of the lowest  $\Lambda$  level, which has the lowest eigen-value  $n = 0$  for the number operator (rather than the energy), can be determined by solving the equation  $\hat{a}\psi_0(z, \bar{\eta}) = 0$ . The solution is given by

$$\psi_0(z, \bar{\eta}) = f(z) \exp\left(\frac{z\bar{\eta}}{2l_b^2}\right), \quad (\text{S16})$$

where  $f(z)$  is an arbitrary holomorphic function of  $z$ . It is convenient to choose  $f_m(z) \propto z^m$ ,  $m \in \mathbb{Z}^+$ , to form a complete basis set for the lowest  $\Lambda$ -level.

Wave functions for higher  $\Lambda$  levels with index  $n > 0$  can be obtained by applying  $\hat{a}^\dagger$  to  $\psi_0(z, \bar{\eta})$ , as shown in the main text. In particular, the wave function of the second  $\Lambda$ -level ( $n = 1$ ) can be written as

$$\psi_n(z, \bar{\eta}) = \hat{a}^\dagger \psi_0(z, \bar{\eta}) \propto \exp\left(\frac{z\bar{\eta}}{2l_b^2}\right) \left(\partial_z - \frac{\bar{\eta}}{l^2}\right) f(z), \quad (\text{S17})$$

where  $l = l_B/\sqrt{\tilde{\nu}\gamma}$  denotes the effective magnetic length of CFs.

### F. Many body CF wave function

Many body CF wave functions  $\Psi_{\text{CF}}(\{z_i, \bar{\eta}_i\})$  are constructed by forming Slater determinants from single-particle CF wave functions. For a fully-occupied lowest ( $n = 0$ )  $\Lambda$ -level, using the complete basis set defined above and Eq. (S16), we have:

$$\Psi_{\text{CF}}^0(\{z_i, \bar{\eta}_i\}) = \prod_{i < j} (z_i - z_j) \prod_i \exp\left(\frac{z_i \bar{\eta}_i}{2l_b^2}\right). \quad (\text{S18})$$



For the many-body CF wave function at  $\nu = 7/3$ , where the second ( $n = 1$ )  $\Lambda$  level is fully occupied, we apply Eq. (S17), and obtain:

$$\Psi_{\text{CF}}(\{z_i, \bar{\eta}_i\}) \propto \prod_i (2l_B^2 \partial_{z_i} - \bar{\eta}_i) \Psi_{\text{CF}}^0(\{z_i, \bar{\eta}_i\}) \quad (\text{S19})$$

$$\propto \prod_i \exp\left(\frac{z_i \bar{\eta}_i}{2l_b^2}\right) \left(2\partial_{z_i} - \frac{\bar{\eta}_i}{l^2}\right) \prod_{i < j} (z_i - z_j). \quad (\text{S20})$$

### G. Electron wave function

The electron wave function is obtained by overlapping  $\Psi_{\text{CF}}$  with the  $1/2$  Laughlin state of vortices [2]. We have:

$$\begin{aligned} \Psi(\{z_i\}) &= \int \prod_i d\mu_b(\boldsymbol{\eta}_i) \Psi_{\text{CF}}(\{z_i, \bar{\eta}_i\}) \prod_{i < j} (\eta_i - \eta_j)^2 \\ &\propto \int \prod_i d\mu_b(\boldsymbol{\eta}_i) \exp\left(\frac{z_i \bar{\eta}_i}{2l_b^2}\right) \left(2\partial_{z_i} - \frac{\bar{\eta}_i}{l^2}\right) \prod_{i < j} (z_i - z_j)(\eta_i - \eta_j)^2. \end{aligned} \quad (\text{S21})$$

To complete the integral, we note that the exponential factor is the complex conjugate of the reproducing kernel of the  $\boldsymbol{\eta}$ -Bergman space Eq. (S8). The integral maps  $\eta_i$  to  $z_i$ , and  $\bar{\eta}_i$  to  $2l_b^2 \partial_{z_i}$ , as indicated by Eqs. (S4, S5). For  $\nu = 7/3$ , we have  $l_b^2/l^2 = 1/2$ . The electron wave function can then be written as:

$$\Psi(\{z_i\}) \propto \lim_{\{\eta_i \rightarrow z_i\}} \prod_i (2\partial_{z_i} - \partial_{\eta_i}) \prod_{i < j} (z_i - z_j)(\eta_i - \eta_j)^2. \quad (\text{S22})$$

### H. Haffnian wave function

To obtain an explicit form of the electron wave function, we first cast Eq. (S22) into the form

$$\Psi(\{z_i\}) \propto \prod_{i < j} (z_i - z_j)^3 \lim_{\eta \rightarrow z} \prod_i (\hat{\mathcal{D}}_i + \mathcal{A}_i), \quad (\text{S23})$$

where we define  $\hat{\mathcal{D}}_i \equiv 2\partial_{z_i} - \partial_{\eta_i}$  and  $\mathcal{A}_i \equiv 2 \sum_{j \neq i} [1/(z_i - z_j) - 1/(\eta_i - \eta_j)]$ .

We then expand the product. Key observations are:

- $\lim_{\eta \rightarrow z} \mathcal{A}_i = 0$ ;
- $\hat{\mathcal{D}}_i \mathcal{A}_j = 4/(z_i - z_j)^2 + 2/(\eta_i - \eta_j)^2$  for  $i \neq j$ ;
- $\hat{\mathcal{D}}_i \hat{\mathcal{D}}_j \mathcal{A}_k = 0$  for  $i \neq j \neq k$ .

Consequently, non-zero combinations from the expansion must pair  $\{\hat{\mathcal{D}}_i\}$  and  $\{\mathcal{A}_i\}$  one by one, giving rise to terms like  $(\hat{\mathcal{D}}_1 \mathcal{A}_2)(\hat{\mathcal{D}}_3 \mathcal{A}_4) \dots$  and its permutations over the indices. Therefore, we have:

$$\Psi(\{z_i\}) \propto \lim_{\eta \rightarrow z} \sum_{\sigma \in P(N)} \prod_i (\hat{\mathcal{D}}_{\sigma(2i-1)} \hat{\mathcal{A}}_{\sigma(2i)}) \propto \sum_{\sigma \in P(N)} \prod_i \frac{1}{(z_{\sigma(2i-1)} - z_{\sigma(2i)})^2}, \quad (\text{S24})$$

where the summation of  $\sigma$  is over  $P(N)$ , the set of all permutations of  $\{1, 2, \dots, N\}$ . The final form is recognized as the Haffnian of a matrix  $\mathcal{M}$  with the non-diagonal matrix elements  $\mathcal{M}_{ij} = 1/(z_i - z_j)^2$ , which is denoted as  $\text{Hf}[1/(z_i - z_j)^2]$  in the main text.

## III. $\Lambda$ -LEVELS FOR $\nu = 12/5$

According to the CF theory, the filling fraction  $\nu = 12/5$  ( $\tilde{\nu} = 2/5$ ) corresponds to a state of  $\text{CF}^2$  with two fully occupied  $\Lambda$ -levels. Applying Eq. (S15) with  $\gamma = 1/2$ , we can determine the energies of  $\Lambda$ -levels for this case. The result is shown in Fig. S1, where the two lowest-energy  $\Lambda$ -levels have the indices  $n = 2$  and  $n = 3$ . This differs from  $\nu = 2/5$ , where  $\text{CF}^2$  occupies levels  $n = 0$  and  $n = 1$ . Consequently, the ground-state wave function for  $\nu = 12/5$  should differ from that for  $\nu = 2/5$ .

Remarkably, the CF theory can predict correctly the distinction between  $\nu = 12/5$  and  $\nu = 11/5$ , despite their proximity. Our analysis suggests that  $\nu = 12/5$  is distinct from its counterpart in the LLL, whereas  $\nu = 11/5$  is not, as it is a state of  $\text{CF}^4$  with a quasiconvex dispersion. This aligns with observations from previous studies.

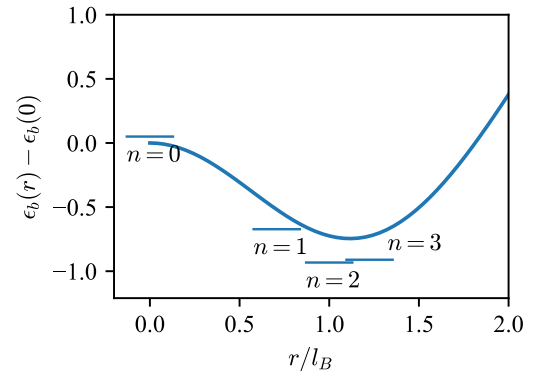


FIG. S1: Energies of  $\Lambda$ -levels for  $\text{CF}^2$  in  $\nu = 12/5$ .

## IV. SPHERICAL GEOMETRY

### A. Landau levels

In the spherical geometry, a magnetic monopole with strength (the total number of magnetic quantum fluxes)  $2Q \in \mathbb{Z}$  is placed at the center of a sphere, generating a uniform magnetic field over its surface. It creates Landau levels on the sphere, which are the eigenstates of the total angular momentum operators  $|\hat{\mathbf{L}}|^2$ . A Landau level, indexed by a non-negative integer  $n \geq 0$ , has the angular momentum quantum number  $l = Q + n$  and degeneracy  $2l + 1$  [4, 5].

The system can be formulated in a form analogue to that of the disk geometry using the stereographic projection [6]

$$z = e^{i\phi} \tan \frac{\theta}{2}, \quad (\text{S25})$$

which maps a point with the polar angles  $(\theta, \phi)$  on a sphere of unit diameter onto a complex plane. We introduce the operator  $\hat{\Pi}_Q \equiv |\hat{\mathbf{L}}|^2 - Q(Q + 1)$ . In terms of the coordinate on the plane, the operator can be written as

$$\hat{\Pi}_Q = -\left(1 + |z|^2\right)^2 \left( \partial_z - Q \frac{\bar{z}}{1 + |z|^2} \right) \left( \partial_{\bar{z}} + Q \frac{z}{1 + |z|^2} \right). \quad (\text{S26})$$

Landau levels are eigenstates of  $\hat{\Pi}_Q$ , with eigenvalues  $l(l + 1) - Q(Q + 1)$ .

The wave functions of the LLL take the general form

$$\psi_0^{(Q)}(z) (1 + |z|^2)^{-Q}, \quad (\text{S27})$$

where  $\psi_0^{(Q)}(z)$  is a holomorphic polynomial in  $z$  with a degree no greater than  $2Q$ . The factor  $(1 + |z|^2)^{-Q}$  is analogous to the Gaussian factor in the wave functions of the disk geometry. A complete basis set for the LLL is given by the polynomials:

$$\psi_{0,m}^{(Q)}(z) \propto z^m, \quad m = 0, 1, 2, \dots, 2Q. \quad (\text{S28})$$

The wave functions of higher Landau levels can be constructed from those of the LLL. For a system with monopole strength  $2Q$ , the Landau level with the index  $n$  has the degeneracy  $2(Q + n) + 1$ , identical to the degeneracy of the LLL for a monopole strength  $2(Q + n)$ . This allows for an one-to-one mapping between their states. The wave function in the  $n$ -th Landau level for monopole strength  $2Q$  takes the form

$$\psi_n^{(Q)}(z) (1 + |z|^2)^{-(Q+n)}. \quad (\text{S29})$$

It can be related to the LLL wave function  $\psi_0^{(Q+n)}(z)$  for monopole strength  $2(Q + n)$  by

$$\psi_n^{(Q)}(z) \propto \left( \prod_{i=1}^n \hat{A}_{2Q+n+i} \right) \psi_0^{(Q+n)}(z), \quad (\text{S30})$$

where

$$\hat{A}_q \equiv (1 + |z|^2)\partial_z - q\bar{z}, \quad q \in \mathbb{Z}^+, \quad (\text{S31})$$

acts as a raising operator for the spherical geometry. The following identity holds:

$$\hat{\Pi}_q \hat{A}_{q+1} = \hat{A}_{q+1} \hat{\Pi}_{q+1} + 2(q+1). \quad (\text{S32})$$

Using the identity, it is straightforward to show that the wave function Eq. (S27) constructed using Eq. (S30) is indeed an eigenstate of  $\hat{\Pi}_Q$  with the expected eigenvalue for the  $n$ -th  $\Lambda$  level.

### B. Bergman space

We can define the Bergman space for the LLL on a sphere. It has the integral measure:

$$d\mu_Q(z) = \frac{(2Q+1) d^2z}{\pi} \left( \frac{1}{1+|z|^2} \right)^{2Q+2}, \quad (\text{S33})$$

and the reproducing kernel

$$K_Q(z, \bar{\xi}) = (1 + z\bar{\xi})^{2Q}. \quad (\text{S34})$$

Projection identities on a sphere analogue to Eq. (S5) read

$$\int d\mu_Q(\xi) K_Q(z, \bar{\xi}) \frac{\bar{\xi}^m}{(1+|\xi|^2)^m} \psi(\xi) = \frac{(2Q+1)!}{(2Q+1+m)!} \partial_z^m \psi(z), \quad (\text{S35})$$

$$\int d\mu_Q(\xi) K_Q(z, \bar{\xi}) \frac{\bar{\xi}^m}{(1+z\bar{\xi})^m} \psi(\xi) = \frac{(2Q-m)!}{(2Q)!} \partial_z^m \psi(z). \quad (\text{S36})$$

### C. $\Lambda$ levels on a sphere

For the dipole model of spherical geometry, we assume a monopole field strength  $2Q$  for electrons and a negative monopole strength  $-2q = -2(N-1)$  for vortices.

In the spherical geometry, just like the disk geometry,  $\Lambda$ -levels can be defined as the eigen-states of the  $\hat{r}^2$  operator, where  $r^2$  is interpreted as the squared chord distance between an electron and a vortex on the surface of the sphere. The squared chord distance can be expressed in terms of the stereographic coordinates of the electron and vortex:

$$r^2 = \frac{|z - \eta|^2}{(1 + |z|^2)(1 + |\eta|^2)}, \quad (\text{S37})$$

The  $\hat{r}^2$  operator is defined through a projection to the CF Bergman space:

$$\hat{r}^2 \psi(z, \bar{\eta}) \equiv \int d\mu_Q(\xi) d\mu_q(\eta') K_Q(z, \bar{\xi}) K_q(\bar{\eta}, \eta') \frac{(\bar{\xi} - \bar{\eta})(\xi - \eta')}{(1 + |\xi|^2)(1 + \bar{\eta}\eta')} \psi(\xi, \bar{\eta}'). \quad (\text{S38})$$

By applying the projection identities Eqs. (S35, S36), we obtain the explicit form of the operator:

$$\hat{r}^2 = -\frac{(1 + z\bar{\eta})^2}{4(Q+1)q} \left( \partial_z - 2Q \frac{\bar{\eta}}{1 + z\bar{\eta}} \right) \left( \partial_{\bar{\eta}} - 2q \frac{z}{1 + z\bar{\eta}} \right). \quad (\text{S39})$$

The  $\hat{r}^2$  operator can be related to the  $\Pi_Q$  operator for ordinary Landau levels with monopole strength  $2Q \equiv 2(Q-q)$  via an orthogonal transformation combined with analytic continuation:

$$\hat{\Pi}_Q \propto (1 + z\bar{\eta})^{-Q-q} \hat{r}^2 (1 + z\bar{\eta})^{Q+q} \Big|_{\bar{\eta} \rightarrow \bar{z}} \quad (\text{S40})$$

Thus, in the spherical geometry, similar to the disk geometry (see Appendix A of Ref. [2]),  $\Lambda$ -level wave functions can be inferred from their Landau-level counterparts using the relation:

$$\psi_{nm}(z, \bar{\eta}) \propto \psi_{nm}^{(Q)}(z, \bar{z}) \Big|_{\bar{z} \rightarrow \bar{\eta}} (1 + z\bar{\eta})^{2q-n}, \quad (\text{S41})$$

where  $\psi_{nm}(z, \bar{\eta})$  denotes a wave function of the  $n$ -th  $\Lambda$ -level, and  $\psi_{nm}^{(Q)}(z, \bar{z})$  a wave function of the  $n$ -th Landau level.

### D. Many body CF wave function

Using Eqs. (S28, S30, S41), we can construct a complete basis set of the second  $\Lambda$ -level as follows:

$$\psi_{1,m}(z, \bar{\eta}) \propto (1 + z\bar{\eta})^{2q-1} [(1 + z\bar{\eta})\partial_z - 2(\mathcal{Q} + 1)\bar{\eta}] z^m \quad (\text{S42})$$

$$= K_q(z, \bar{\eta}) \left( \partial_z - \frac{2(\mathcal{Q} + 1)\bar{\eta}}{1 + z\bar{\eta}} \right) z^m, \quad (\text{S43})$$

where we  $K_q(z, \bar{\eta})$  is the reproducing kernel defined in Eq. (S34).

The many body CF wave function  $\Psi_{\text{CF}}(\{z_i, \bar{\eta}_i\})$  for a fully occupied second ( $n = 1$ )  $\Lambda$ -level is then written as

$$\Psi_{\text{CF}}(\{z_i, \bar{\eta}_i\}) \propto \prod_i K_q(z_i, \bar{\eta}_i) \left[ \partial_{z_i} - \frac{2(\mathcal{Q} + 1)\bar{\eta}_i}{1 + z_i\bar{\eta}_i} \right] \prod_{i < j} (z_i - z_j). \quad (\text{S44})$$

### E. Electron wave function

The corresponding electron wave function is given by

$$\Psi(\{z_i\}) \propto \int \prod_i d\mu_q(\boldsymbol{\eta}_i) K_q(z_i, \bar{\eta}_i) \left[ \partial_{z_i} - \frac{2(\mathcal{Q} + 1)\bar{\eta}_i}{1 + z_i\bar{\eta}_i} \right] \prod_{i < j} (z_i - z_j)(\eta_i - \eta_j)^2. \quad (\text{S45})$$

By applying Eq. (S36), it simplifies to

$$\Psi(\{z_i\}) \propto \lim_{\{\eta_i \rightarrow z_i\}} \prod_i \left[ \partial_{z_i} - \frac{\mathcal{Q} + 1}{q} \partial_{\eta_i} \right] \prod_{i < j} (z_i - z_j)(\eta_i - \eta_j)^2. \quad (\text{S46})$$

For a fully occupied second  $\Lambda$ -level, we have  $2\mathcal{Q} + 3 = N$ , and using the identity  $q = (N - 1)$ , it follows  $(\mathcal{Q} + 1)/q = 1/2$ . The wave function then reduces to a form that is identical to Eq. (S22).

## V. EXACT DIAGONALIZATIONS

### A. Disk geometry

We simulate a system of  $N$  interacting electrons on a disk of radius  $R_c \equiv \sqrt{2N/\tilde{\nu}}$  (with  $l_B = 1$ ). The disk contains a neutralizing positive charge background with a uniform charge density within  $R_c$ . The presence of the neutralizing charge background induces a single-body potential,  $\Phi(r)$ , experienced by electrons.

Exact diagonalizations are performed in a finite Hilbert space spanned by the basis set  $\phi_m(z) = z^m/\sqrt{m!}$ , with  $m < \tilde{\nu}^{-1}N + D$  and  $D \in \mathbb{Z}^+$ . This allows electrons to extend beyond the disk radius by  $D$  additional orbits. For the results presented in the main text, we set  $D = 5$ .

The interaction matrix elements can be determined analytically. For the LLL, the explicit form for the Coulomb interacting matrix elements,  $V_{m_1 m_2 m_3 m_4}$ , is provided in Ref. 7. For the 1LL, the matrix elements  $\tilde{V}_{m_1 m_2 m_3 m_4}$  of the effective interaction can be expressed in terms of  $V_{m_1 m_2 m_3 m_4}$  as follows:

$$\begin{aligned} \tilde{V}_{m_1 m_2 m_3 m_4} = & \sqrt{(m_1 + 1)(m_3 + 1)} \left( \sqrt{(m_2 + 1)(m_4 + 1)} V_{m_1+1, m_2+1, m_3+1, m_4+1} - (m_2 + m_4) V_{m_1+1, m_2, m_3+1, m_4} \right. \\ & \left. + \sqrt{m_2 m_4} V_{m_1+1, m_2-1, m_3+1, m_4-1} \right) \\ & - (m_1 + m_3) \left( \sqrt{(m_2 + 1)(m_4 + 1)} V_{m_1, m_2+1, m_3, m_4+1} - (m_2 + m_4) V_{m_1 m_2 m_3 m_4} + \sqrt{m_2 m_4} V_{m_1, m_2-1, m_3, m_4-1} \right) \\ & + \sqrt{m_1 m_3} \left( \sqrt{(m_2 + 1)(m_4 + 1)} V_{m_1-1, m_2+1, m_3-1, m_4+1} - (m_2 + m_4) V_{m_1-1, m_2, m_3-1, m_4} \right. \\ & \left. + \sqrt{m_2 m_4} V_{m_1-1, m_2-1, m_3-1, m_4-1} \right). \end{aligned} \quad (\text{S47})$$

The relation can be derived from the connection between the single-particle electron wave function  $\psi_{1m}(z)$  in the 1LL and its counterparts in the LLL  $\psi_{0m}(z) \equiv \phi_m(z)$ :  $\psi_{1m}(z) = \bar{z}\psi_{0m}(z)/\sqrt{2} - \sqrt{m}\psi_{0, m-1}(z)$ .

Hamiltonian matrices are constructed using the interaction matrix elements and the single-particle potential  $\Phi(r)$ , which is diagonal in the basis set  $\{\phi_m\}$ . The resulting matrices are then diagonalized using the Lanczos algorithm.

It is necessary to test our calculations under different simulation setups, as the disk geometry introduces boundary effects that may influence the results. Two factors can be identified: (i) the charge distribution of the neutralizing background near the boundary, and (ii) the value of  $D$  which determines the number of basis states used in ED. For (i), we smear the abrupt change in the neutralizing charge density at  $R_c$  by assuming that the background has the charge distribution:

$$\rho_b(r) = \rho_0 \frac{\Gamma\left(\frac{R_c^2}{2\lambda^2}, \frac{r^2}{2\lambda^2}\right)}{\Gamma\left(\frac{R_c^2}{2\lambda^2}\right)}, \quad (\text{S48})$$

where  $\Gamma(x, y)$  is the upper incomplete gamma function, and  $\Gamma(x) \equiv \Gamma(x, 0)$  is the complete gamma function. This results in a smooth decrease in density near the boundary over a length scale  $\sim \lambda$ . For (ii), we perform calculations for various values of  $D$ .

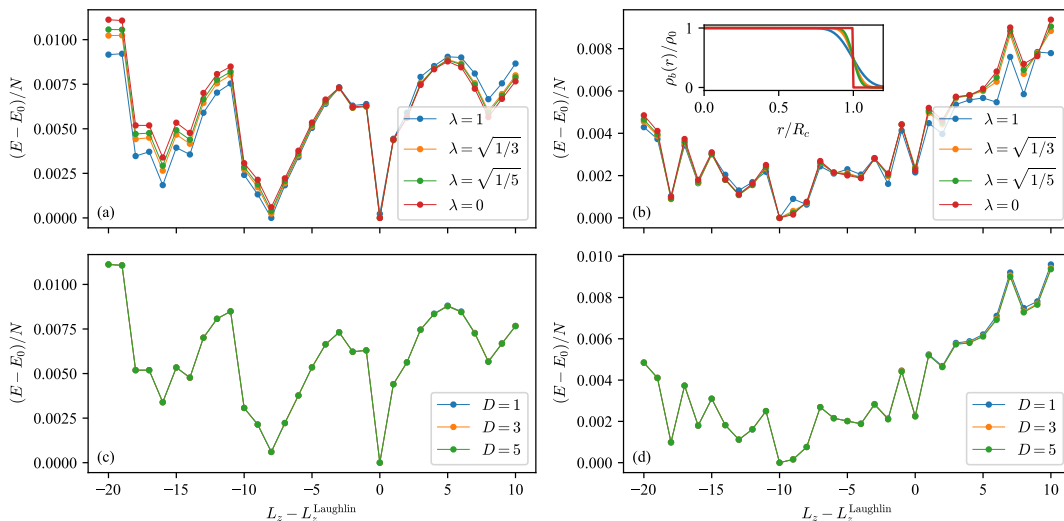


FIG. S2: ED ground state energies for different simulation parameters with  $N = 10$ . (a) and (b) show results for varying values of  $\lambda$ , while (c) and (d) present results for different values of  $D$ . Results for the LLL are displayed in the left [(a) and (c)], and for the 1LL in the right [(b) and (d)].

ED results for various values of  $\lambda$  and  $D$  are shown in Fig. S2. It is evident that these parameters have only minor effects on the results. Our main conclusion that the ground states for  $\nu = 1/3$  and  $\nu = 7/3$  have different expectation values of  $L_z$  remains unaffected by the choice of simulation parameters.

## B. Spherical geometry

Simulating the system on a sphere removes the need for a neutralizing charge background and eliminates boundary effects, making it preferable to disk simulations. However, electron states on a sphere depends on the topological shift  $S$ , requiring us to test various  $(N, S)$  pairs. The results are presented in the main text.

Hamiltonian matrices are constructed using the Coulomb interaction matrix elements, for both the LLL and 1LL, as given in Ref. 4. Resulting Hamiltonian matrices are then diagonalized using the Lanczos algorithm.

## VI. $\text{CF}^2$ IN A FINITE-WIDTH QUANTUM WELL

In Fig. S3, we present the dispersions of  $\text{CF}^2$  in a finite-width quantum well for different values of the width parameter  $w$  (see the main text). As  $w$  increases, the dispersion of CFs evolves from non-quasiconvex to quasiconvex. The transition occurs at  $w \approx 0.7l_B$ , as shown in the right panel of Fig. S3, where the energies of the first and second  $\Lambda$  levels becomes degenerate.

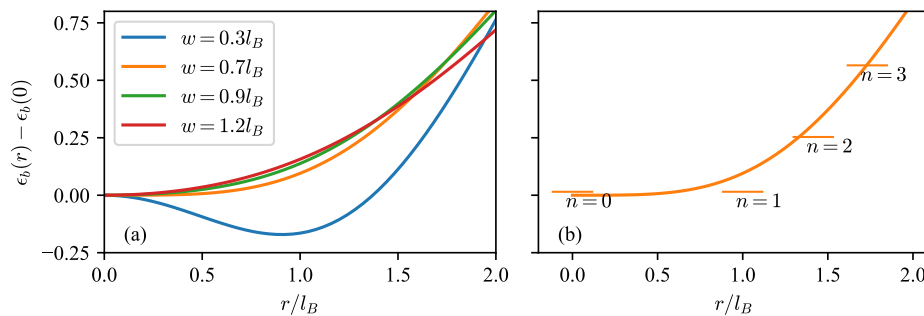


FIG. S3: (a) Dispersions of  $\text{CF}^2$  in the 1LL with different values of  $w$ . (b) Dispersion and energies of  $\Lambda$  levels with  $w = 0.7l_B$ . The energies are in units of  $\tilde{\nu}e^2/16\pi^2\epsilon l_B$ .

## VII. SELF-CONSISTENT DETERMINATION OF THE CF DISPERSION

In the main text, we determine the dispersions of  $\text{CF}^2$  for both the LLL and 1LL by assuming that electrons are in the  $1/3$  Laughlin state. While this is self-consistent for the LLL, it is not for the 1LL, as its CF dispersion suggests that  $\nu = 7/3$  corresponds to a fermionic Haffnian state. Ideally, to achieve full self-consistency, the dispersion should also be determined using the Haffnian state.

Following the mean-field approach developed in Sec. VB of Ref. 2, we determine the electron wave function in the presence of a vortex at the origin:

$$\begin{aligned} \Psi_0^v(\{z_i\}) &= \int \prod_i d\mu(\eta_i) \eta_i^2 \Psi_{\text{CF}}(\{z_i, \bar{\eta}_i\}) \prod_{i<j} (\eta_i - \eta_j)^2 \\ &\propto \lim_{\{\eta_i \rightarrow z_i\}} \prod_i (2\partial_{z_i} - \partial_{\eta_i}) \prod_{i<j} (z_i - z_j)(\eta_i - \eta_j)^2 \prod_i \eta_i^2, \end{aligned} \quad (\text{S49})$$

where  $\Psi_{\text{CF}}(\{z_i, \bar{\eta}_i\})$  is given by Eq. (S20). The electron density profile in the vicinity of the vortex can then be determined.

Following the steps outlined in Sec. II, we obtain the explicit form of the wave function:

$$\Psi_0^v(\{z_i\}) \propto \text{IHf}(\mathcal{M}) \prod_i z_i^2 \prod_{i<j} (z_i - z_j)^3, \quad (\text{S50})$$

where  $\mathcal{M}$  is a matrix with elements  $\mathcal{M}_{ij} = 1/(z_i - z_j)^2$  for  $i \neq j$ , and  $\mathcal{M}_{ii} = -\sqrt{2/3}/z_i$ .  $\text{IHf}(\mathcal{M})$  denotes the loop Haffnian of the matrix [8]. The particular loop Haffnian can also be written as a determinant:  $\text{IHf}(\mathcal{M}) = \det(\tilde{\mathcal{M}})$ , where  $\tilde{\mathcal{M}}$  is a matrix with elements  $\tilde{\mathcal{M}}_{ij} = 1/(z_i - z_j)$  for  $i \neq j$ , and  $\tilde{\mathcal{M}}_{ii} = -\sqrt{2/3}/z_i$ .

In Fig. S4, we present the CF dispersion and  $\Lambda$  level energies computed using the loop Haffnian wave function. The dispersion is quasiconvex and exhibits a steep increase with  $r$ . This is markedly different from the dispersion obtained when assuming the Laughlin wave function.

We attribute the failure to the inadequacy of the mean-field approach, which neglects the exchange symmetry between CFs. The resulting absence of Pauli exclusion induces the issue, which is further amplified by the pairing nature of the Haffnian state. To illustrate, consider the expansion of the loop Haffnian by its diagonal elements:

$$\text{IHf}(\mathcal{M}) = \sum_{s=0}^N \sum_{\{i_1, i_2, \dots, i_s\}} \frac{1}{z_{i_1}} \cdots \frac{1}{z_{i_s}} \times \text{Hf}(m_{\{i_1, i_2, \dots, i_s\}}), \quad (\text{S51})$$

where  $\{i_1, i_2, \dots, i_s\}$  denotes a list of distinct indices,  $m_{\{i_1, i_2, \dots, i_s\}}$  is the matrix obtained by removing the columns and rows with indices  $i_1, i_2, \dots, i_s$  in  $\mathcal{M}$ . The factor  $1/z_{i_1} \cdots 1/z_{i_s}$  indicates that there are  $s$  additional electrons which have pairing correlations with the vortex at the origin, despite the vortex already being bound to an electron which is not included in  $\Psi_0^v$ , according to the assumption of the mean-field approach. This is obviously an artifact that arises from the lack of Pauli-exclusion between the vortex-bound electron and other electrons in the system. Its impact is exacerbated by the  $1/z$  correlation, which is absent in the Laughlin wave function.

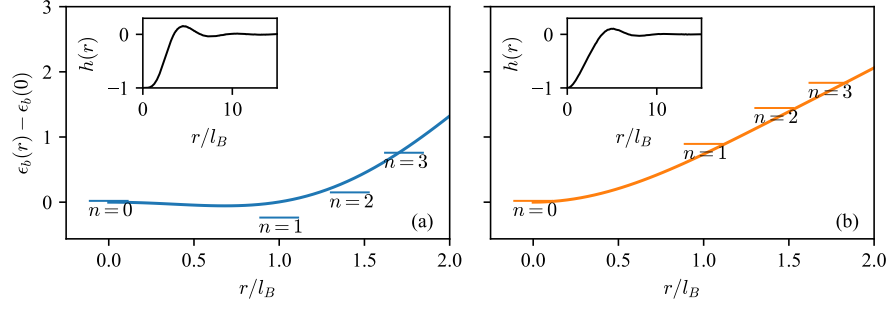


FIG. S4: (a)  $h(r)$ ,  $\epsilon_b(r)$  and  $\Lambda$  levels of the  $7/3$  state based on Eq. (S52). (b) Same as (a) but  $\Psi_0^v(\{z_i\})$  is given by Eq. (S50). The energies are in units of  $\tilde{\nu}e^2/16\pi^2\epsilon l_B$ .

To estimate the CF dispersion for the Haffnian state, we discard the terms with  $s \neq 0$  in the expansion Eq. (S51), as these are considered unphysical. The resulting wave function with a vortex is:

$$\Psi_0^v(\{z_i\}) = \prod_i z_i^2 \Psi^{\text{Hf}}(\{z_i\}), \quad (\text{S52})$$

where  $\Psi^{\text{Hf}}(\{z_i\})$  is the fermionic Haffnian wave function (Eq. [4] of the main text). The corresponding CF dispersion and  $\Lambda$  level energies are shown in Fig. S4 (a). The dispersion determined using the Haffnian wave-function is indeed non-quasiconvex, although the minimum is significantly shallower compared to that determined using the Laughlin wave function.

Properly determining the CF dispersion for the Haffnian state may require an improved mean field approach, e.g., a Hartree-Fock theory for CFs, which fully accounts for the exchange symmetry.

- 
- [1] J. K. Jain and R. K. Kamilla, *Int. J. Mod. Phys. B* **11**, 2621 (1997).
  - [2] J. Shi, *Phys. Rev. Res.* **6**, 023306 (2024).
  - [3] J. König and A. Hucht, *SciPost Phys.* **10**, 007 (2021).
  - [4] J. K. Jain, *Composite fermions* (Cambridge University Press, 2007).
  - [5] F. D. M. Haldane, *Phys. Rev. Lett.* **51**, 605 (1983).
  - [6] G. V. Dunne, *Annals of Physics* **215**, 233 (1992).
  - [7] E. Tsiper, *Journal of Mathematical Physics* **43**, 1664 (2002).
  - [8] A. Björklund, B. Gupt, and N. Quesada, A faster hafnian formula for complex matrices and its benchmarking on a super-computer (2019), arXiv:1805.12498 .